SVENSKA GEOFYSISKA FÖRENINGEN

VOLUME 2, NUMBER 4 **Tellus** NOVEMBER 1950

A QUARTERLY JOURNAL OF GEOPHYSICS

Numerical Integration of the Barotropic Vorticity Equation

By J. G. CHARNEY, R. FJÖRTOFT[1], J. von NEUMANN

The Institute for Advanced Study, Princeton, New Jersey[2]

(Manuscript received 1 November 1950)

Abstract

A method is given for the numerical solution of the barotropic vorticity equation over a limited area of the earth's surface. The lack of a natural boundary calls for an investigation of the appropriate boundary conditions. These are determined by a heuristic argument and are shown to be sufficient in a special case. Approximate conditions necessary to insure the mathematical stability of the difference equation are derived. The results of a series of four 24-hour forecasts computed from actual data at the 500 mb level are presented, together with an interpretation and analysis. An attempt is made to determine the causes of the forecast errors. These are ascribed partly to the use of too large a space increment and partly to the effects of baroclinicity. The rôle of the latter is investigated in some detail by means of a simple baroclinic model.

I. Introduction

Two years ago the Meteorological Research Group at the Institute for Advanced Study adopted the general plan of attacking the problem of numerical weather prediction by a step by step investigation of a series of models approximating more and more the real state of the atmosphere. In accordance with this plan the two-dimensional barotropic model was chosen as the first object of study. The first two publications[3] dealt with the numerical properties of the linearized barotropic equations as a preparation for the numerical integration of the non-linear equations. Such integrations have now been performed and will be described in the present article.

These integrations would not have been possible without the use of a high-speed large-capacity computing instrument. We should like, therefore, to express our warmest thanks to the U. S. Army Ordnance Department and the administration of the Ballistic Research Laboratories in Aberdeen, Maryland for having generously given us the use of their electronic computing machine (The Eniac [compare footnote 5]). The request for the use of the Eniac was made on our behalf by the U. S. Weather Bureau and we should like to thank them also for their gratifying interest and support.

The reasons for regarding the integration of the barotropic equations as an essential

[1] On leave from Det Norske Meteorologiske Institutt, Oslo, Norway.

[2] This work was prepared under Contract N-6-ori-139 with the Office of Naval Research.

[3] CHARNEY (1949), CHARNEY and ELIASSEN (1949).

first step of the general program are as follows: (1) An accumulation of evidence indicates first that the effects of baroclinicity do not manifest themselves in a steady, widespread conversion of potential into kinetic energy, but rather in sporadic and violent local overturnings accompanying what, for want of a better term, may be called baroclinic instability, and second, that when these effects are not predominant, the motion is quasi-barotropic. It is hoped therefore that the barotropic predictions, by their agreements and disagreements with observation, will provide a basis for an a priori classification of the large-scale atmospheric motions. One has the suspicion that certain processes which have heretofore been classed as baroclinic will be found to have a barotropic explanation. (2) If the barotropic forecasts are found to be sufficiently accurate approximations to the upper flow, it is possible that they can be profitably incorporated into practical forecast procedure. (3) Just as the analysis of the linearized barotropic equations served as a pilot study for the integration of the non-linear barotropic equations, so will these integrations supply the necessary background for the treatment of the three-dimensional equations.

The most easily integrated of the barotropic equations are the *primitive* Eulerian equations, in which the local time derivatives of the field variables are given explicitly in terms of their space derivatives. Although the virtual unobservability of the geostrophic deviation and the horizontal divergence renders the initial time derivatives in the Eulerian equations highly inaccurate, the indications are that, contrary to an earlier impression[4], the error will occur only as a small amplitude gravitational oscillation about an essentially correct large-scale flow — providing the space and time increments in the finite difference equations are chosen to satisfy the Courant-Friedrichs-Lewy condition (1928) for the computational stability of the equation governing the motion of long gravity waves. However two main considerations led the writers to decide against attempting the integration of the Eulerian equations at this time. First, the computational stability condition states that the ratio of the space to the time difference must exceed the gravitational wave velocity, about 300 m sec^{-1}, and demands a time increment of some 15 minutes or less. This means that a twenty-four hour forecast would require nearly 100 time cycles for the integration, a formidable number for the machine that was available to the writers. Then there was also the difficulty that the characteristic property of large-scale non-divergent barotropic motions, the conservation of absolute vertical vorticity, is obscured in the integration of the Eulerian equations — which apply as well to the divergent gravity motions — and the results thereby made extremely difficult to analyse and interpret. These difficulties having been regarded by the authors as serious, it was decided instead to base the computation on the quasi-geostrophic, non-divergent vorticity equation, in which the sole dependent variable is the height z of a fixed isobaric surface.

Because of the elliptic character in $\frac{\partial z}{\partial t}$ of the non-divergent vorticity equation, z and certain of its space derivatives must be specified as functions of time at the boundary of a limited forecast region. Since these quantities are known only initially, one has to fix their values in a more or less arbitrary manner, and it becomes necessary to know how rapidly influences from the boundary propagate into the forecast region. This problem has been treated by CHARNEY (1949) who arrived at the conclusion that large-scale influences travel with a speed not radically different from that of the wind, and these influences consequently are provided for by integrating over an area not much larger than the forecast region. Although it is immaterial what values are prescribed at the boundary, it is nevertheless important that the mathematical form of the boundary conditions be known. Experience has shown that a violation of these conditions may lead to errors adjacent to the boundary which propagate into the interior with destructive effect. Since one is dealing with boundaries at which the conditions are not naturally prescribed by the geometry of the motion, as for example at a wall, it is not immediately obvious what these conditions are. A heuristic argument will be advanced to show

4 CHARNEY (1949, p. 12).

that the following are probably correct: where fluid is entering the region enclosed by the boundary both z and the relative vorticity must be prescribed, but where fluid is leaving the region it is enough to prescribe z.

The first part of the following discussion, the mathematical part, is devoted to the treatment of the boundary conditions, the method of solution of the finite-difference vorticity equation, and the computational stability criteria. The second part contains a description and analysis of the results of four twenty-four hour forecasts computed from actual data and a final section devoted to an account of a baroclinic model which is used to explain some of the barotropic forecast discrepancies.

II. The Vorticity Equation

We assume that the horizontal winds in the large-scale systems vary according to the law

$$\mathbf{v}(s_1, s_2, p) = A(p)\ \mathbf{v}(s_1, s_2, p_0) \tag{1}$$

where s_1, s_2 are orthogonal curvilinear distance co-ordinates on the sphere, p is the vertical pressure co-ordinate, and p_0 the mean surface value of p. If a bar denotes a vertical pressure average, i.e.,

$$\overline{\alpha} = \frac{1}{p_0}\int_0^{p_0} \alpha\, dp, \tag{2}$$

the integrated vorticity equation takes the approximate form (CHARNEY [1949, p. 383])

$$\frac{\partial \overline{\zeta}}{\partial t} = -\overline{\mathbf{v}} \cdot \nabla (K\overline{\zeta} + f), \tag{3}$$

where $\overline{\zeta}$ is the mean relative vertical vorticity component, f is the coriolis parameter, and $K = \overline{A^2}/(\overline{A})^2$.

If $A^\star$ is defined by

$$A^\star = \overline{A^2}/\overline{A}$$

and (3) is multiplied by $A^\star/\overline{A}$ we obtain

$$\frac{\partial \zeta^\star}{\partial t} = -\mathbf{v}^\star \cdot \nabla (\zeta^\star + f), \tag{4}$$

where $\mathbf{v}^\star$ and $\zeta^\star$ are respectively the wind velocity and relative vorticity at the level $p^\star$ defined by $A(p^\star) = A^\star$. Since approximately

$$\frac{d}{dt}(\zeta + f) = \frac{\partial \zeta}{dt} + \mathbf{v} \cdot \nabla (\zeta + f) = \\ = -(\zeta + f)\ \mathrm{div}\ \mathbf{v}, \tag{5}$$

$p^\star$ is the level of non-divergence. It is known (CHARNEY [*loc. cit.*]) that $\overline{p}$, the level at which $A = \overline{A}$ and $\mathbf{v} = \overline{\mathbf{v}}$, is between 600 and 500 mb and that $\overline{A^2}/\overline{A}^2$ is approximately 1.25. Hence we have

$$\frac{|\mathbf{v}^\star|}{|\overline{\mathbf{v}}|} = \frac{A^\star}{\overline{A}} = \frac{\overline{A^2}}{\overline{A}^2} = 1.25$$

and from the average variation of $\mathbf{v}$ with height we find that $p^\star$ is approximately 100 mb higher than $\overline{p}$ or between 500 and 400 mb. We shall take this level to be 500 mb in the forecasts.

Evaluating the vorticity of the geostrophic wind

$$\mathbf{v}^\star = -\frac{g}{f}\,\mathbf{k} \times \nabla z, \tag{6}$$

where $\mathbf{k}$ is the unit vertical vector and z the height of the $p^\star$ surface, we find

$$\zeta^\star \approx \frac{g}{f}\,\mathrm{div}\,\nabla z \equiv \frac{g}{f}\,\Delta_s z, \tag{7}$$

and substituting this expression into (4) we obtain the quasi-geostrophic vorticity equation:

$$\frac{\partial}{\partial t}(\Delta_s z) = \frac{\partial \eta}{\partial s_1}\frac{\partial z}{\partial s_2} - \frac{\partial \eta}{\partial s_2}\frac{\partial z}{\partial s_1} = J_s(\eta, z), \tag{8}$$

where η is the absolute vorticity

$$\eta = \frac{g}{f}\,\Delta_s z + f. \tag{9}$$

Here Δ_s is the surface spherical Laplacian operator, and J_s is the Jacobian of η and z with respect to s_1 and s_2. Equation (8) is taken to be the basic equation governing the large-scale motions in a barotropic atmosphere. Its solution may be found iteratively by solving

for $\frac{\partial z}{\partial t}$ and extrapolating the motion forward in time, but for this purpose the boundary conditions must first be ascertained.

III. The Boundary Conditions

Let R be a region of the earth bounded by the simple, closed, rectifiable curve C. If $\Delta_s z$ is known in R and z is given on C, z may be obtained in R by solving a Poisson's equation. Hence, if the boundary conditions are prescribed in such a way that z is always known on C and $\Delta_s z$ is known in R, the solution to (8) for the region R will be determined. Suppose now that z is a given function of time on C, so that the tangential derivative and therefore the normal velocity is fixed, and that we know its values initially in R. Since according to (4) the absolute vorticity is advected with the fluid, after a small time δt the distribution of $\Delta_s z$ will be known everywhere in R except in the part, δR, which is penetrated by fluid from outside. If in addition $\Delta_s z$ had been prescribed on that part of C where fluid was entering, we should also have been able to say exactly what vorticity had entered δR, since the normal velocity on C is known. Hence we may assert that *the motion is determined by the specification of z everywhere on the boundary, and the vorticity on that part of the boundary at which fluid is entering the interior region.*

To supplement the foregoing heuristic argument we now give a demonstration of the sufficiency of these boundary conditions in the case of a special two-dimensional nondivergent flow which, however, appears to exhibit the essential mathematical properties of the barotropic flow. It will also be shown that the specification of only the stream function does not determine the motion.

We consider the two-dimensional incompressible motion of an inviscid fluid on a circular cylinder, in which the force of gravity is directed radially inward so that no external forces act along its surface. Let y be directed along the axis of the cylinder and x be directed at right angles to y. Because of the incompressibility assumption we may introduce a stream function ψ and write for the vorticity equation

$$\frac{\partial}{\partial t}(\Delta\psi) = \frac{\partial}{\partial x}(\Delta\psi)\frac{\partial\psi}{\partial y} - \frac{\partial}{\partial y}(\Delta\psi)\frac{\partial\psi}{\partial x}, \tag{10}$$

an equation corresponding closely to (8).

Consider the ring shaped domain bounded by the two circles $y = 0$ and $y = a$ and prescribe the boundary conditions $\psi = x$ on each circle for all $t > 0$. Also let $\psi = x$ in the entire domain at $t = 0$. The motion consists initially of a uniform streaming parallel to the y-axis. It may easily be verified that there are an infinity of solutions of (10) satisfying the initial and boundary conditions of the form

$$\psi = x + [\beta(t) - \beta(t-a)]\frac{y}{a} - [\beta(t) - \beta(t-y)], \tag{11}$$

where β is limited solely by the requirement

$$\beta(t) = 0 \text{ for } t \leqq 0. \tag{12}$$

It is clear, therefore, that a knowledge of ψ in the boundary does not determine the motion. But the motion *is* determined if $\Delta\psi$ is also specified on the boundary where fluid is entering, i.e., at $y = 0$: Let $(\Delta\psi)_{y=0} = F(t)$, then from (11) and (12)

$$(\Delta\psi)_{y=0} = \frac{d^2\beta(t)}{dt^2} = F(t),$$

and

$$\beta(t) = \int_0^t \int_0^a F(\gamma)\, d\gamma\, d\alpha + At = G(t) + At,$$

where A is an arbitrary constant. Substitution of this expression into (11) gives

$$\psi = x + [G(t) - G(t-a)]\frac{y}{a} - [G(t) - G(t-a)],$$

and ψ is completely determined.

IV. The Solution of the Vorticity Equation

The following method of solving the finite difference vorticity equation is well-adapted to a variety of high-speed computing machines, although it was chosen specifically for use on

the Eniac.[5] It is not, however, recommended for hand computation.

The spherical earth is first mapped conformally onto a plane. If m is the magnification factor, the Laplacian and Jacobian operators transform as follows:

$$\Delta_s = m^2\Delta;\ J_s = m^2 J$$

where Δ and J are the Laplacian and Jacobian on the plane. Thus (8) is transformed into

$$\left.\begin{aligned} \frac{\partial}{\partial t}(\Delta z) &= J(\eta, z) \\ \eta &= h\Delta z + f \end{aligned}\right\} \qquad (13)$$

with

$$h = \frac{gm^2}{f}. \qquad (14)$$

The mapping used for the numerical integrations was the stereographic projection of the earth's surface onto a plane tangent at the north pole. In this case we have the following relation between the geographical latitude φ and the distance r from the pole on the map:

$$r = \frac{\cos\varphi}{1 + \sin\varphi},$$

where the radius of the equator on the map is chosen as the unit of distance. We obtain

$$\left.\begin{aligned} m &= -\frac{dr}{\frac{1}{2}d\varphi} = \frac{2}{1+\sin\varphi} = 1 + r^2 \\ f &= 2\Omega\sin\varphi = 2\Omega\,\frac{1-r^2}{1+r^2} \\ h &= \frac{gm^2}{f} = \frac{g}{2\Omega}\,\frac{(1+r^2)^3}{1-r^2} \end{aligned}\right\}, \qquad (15)$$

where Ω is the earth's angular speed of rotation. With the notation

$$\xi = \Delta z$$

the system (13) is replaced by

$$\left.\begin{aligned} \eta &= h\xi + f \\ \frac{\partial\xi}{\partial t} &= J(\eta, z) \\ \Delta\left(\frac{\partial z}{\partial t}\right) &= \frac{\partial\xi}{\partial t} \end{aligned}\right\}, \qquad (16)$$

Since it is immaterial what values are assigned to z and Δz on the boundary, as long as it is sufficiently far removed from the forecast region, we may prescribe the conditions

$$\left.\begin{aligned} \frac{\partial z}{\partial t} &= 0, \\ \frac{\partial\xi}{\partial t} &= 0 \text{ for } z_{ta} \geq 0, \end{aligned}\right\} \qquad (17)$$

where z_{ta} is the tangential derivative of z taken in the direction that has the interior of the region on the left.

For simplicity a rectangular area with sides L_x and L_y is chosen, and a rectangular grid of points is defined by the co-ordinates $x = \frac{L_x}{p} i$, $y = \frac{L_y}{q} j$ $(i = 0, 1, \ldots, p;\ j = 0, 1, \ldots, q)$ with boundary lines $i = 0$, $i = p$ and $j = 0$, $j = q$. The grid intervals $\frac{L_x}{p}$ and $\frac{L_y}{q}$ are taken to be equal to the common value Δs.

The quantities h and f are independent of t and may be determined once and for all from (15) and

$$r^2 = (x - x_p)^2 + (y - y_p)^2$$

where x_p and y_p are the co-ordinates of the pole.

Using centered space differences and denoting by the subscript ij the value of a quantity at the point (i, j), we derive the finite difference analogue of (16),

5 *Electronic Numerical Integrator and Computer*, Ballistic Research Laboratories, Aberdeen Proving Ground, Maryland.

$$\left.\begin{aligned} \eta_{ij} &= h_{ij}\,\xi_{ij} + f_{ij} \\ \frac{\partial \xi_{ij}}{\partial t} &= J_{ij}(\eta, z) \\ \Delta_{ij}\left(\frac{\partial z}{\partial t}\right) &= -\frac{\partial \xi_{ij}}{\partial t}, \end{aligned}\right\} \tag{18}$$

where

$$\Delta_{ij}\left(\frac{\partial z}{\partial t}\right) = \frac{1}{(\triangle s)^2}\left[\left(\frac{\partial z}{\partial t}\right)_{i+1j} + \left(\frac{\partial z}{\partial t}\right)_{i-1j} + \left(\frac{\partial z}{\partial t}\right)_{ij+1} + \left(\frac{\partial z}{\partial t}\right)_{ij-1} - 4\left(\frac{\partial z}{\partial t}\right)_{ij}\right],$$

$$J_{ij}(\eta, z) = \frac{1}{4(\triangle s)^2}\left[(\eta_{i+1j} - \eta_{i-1j})(z_{ij+1} - z_{ij-1}) - (\eta_{ij+1} - \eta_{ij-1})(z_{i+1j} - z_{i-1j})\right]$$

The solution of (18) for the boundary condition

$$\left(\frac{\partial z}{\partial t}\right)_{oj} = \left(\frac{\partial z}{\partial t}\right)_{pj} = \left(\frac{\partial z}{\partial t}\right)_{io} = \left(\frac{\partial z}{\partial t}\right)_{iq} = 0; \quad (i = 0, 1, \ldots, p;\ j = 0, 1, \ldots q) \tag{19}$$

is then given explicitly by

$$\left(\frac{\partial z}{\partial t}\right)_{ij} = -\frac{(\triangle s)^2}{pq}\sum_{l=1}^{p-1}\sum_{m=1}^{q-1}\sum_{r=1}^{p-1}\sum_{s=1}^{q-1}\left(\sin^2\frac{\pi l}{2p} + \sin^2\frac{\pi m}{2q}\right)^{-1}\left(\frac{\partial \xi}{\partial t}\right)_{rs} \sin\frac{\pi l r}{p}\sin\frac{\pi m s}{q}\sin\frac{\pi l i}{p}\sin\frac{\pi m j}{q} \tag{20}$$

The boundary values of $\frac{\partial \xi}{\partial t}$ require special attention. Here we make use of the second condition in (17): if fluid is entering the rectangle, we set $\frac{\partial \xi}{\partial t} = 0$; if fluid is leaving, $\frac{\partial \xi}{\partial t}$ is determined by the interior values of η and z. In the latter case we shall agree to extrapolate $\frac{\partial \xi}{\partial t}$ linearly from the interior. This leads to the following scheme:

$$\left.\begin{aligned} &i = 0\colon z_{oj+1} - z_{oj-1} && \begin{cases} \geq 0, & \left(\frac{\partial \xi}{\partial t}\right)_{oj} = 2\left(\frac{\partial \xi}{\partial t}\right)_{1j} - \left(\frac{\partial \xi}{\partial t}\right)_{2j} \\ < 0, & \left(\frac{\partial \xi}{\partial t}\right)_{oj} = 0 \end{cases} \\ &i = p\colon z_{pj-1} - z_{pj+1} && \begin{cases} \geq 0, & \left(\frac{\partial \xi}{\partial t}\right)_{pj} = 2\left(\frac{\partial \xi}{\partial t}\right)_{p-1j} - \left(\frac{\partial \xi}{\partial t}\right)_{p-2j} \\ < 0, & \left(\frac{\partial \xi}{\partial t}\right)_{pj} = 0 \end{cases} \\ &j = 0\colon z_{i-1o} - z_{i+1o} && \begin{cases} \geq 0 & \left(\frac{\partial \xi}{\partial t}\right)_{io} = 2\left(\frac{\partial \xi}{\partial t}\right)_{i1} - \left(\frac{\partial \xi}{\partial t}\right)_{i2} \\ < 0 & \left(\frac{\partial \xi}{\partial t}\right)_{io} = 0 \end{cases} \\ &j = q\colon z_{i+1q} - z_{i-1q} && \begin{cases} \geq 0 & \left(\frac{\partial \xi}{\partial t}\right)_{iq} = 2\left(\frac{\partial \xi}{\partial t}\right)_{iq-1} - \left(\frac{\partial \xi}{\partial t}\right)_{iq-2} \\ < 0 & \left(\frac{\partial \xi}{\partial t}\right)_{iq} = 0 \end{cases} \end{aligned}\right\} \tag{21}$$

The corner points are exceptional, but as they are not required in the computation they need not be considered.

Having determined $\left(\frac{\partial \xi}{\partial t}\right)_{ij}$ and $\left(\frac{\partial z}{\partial t}\right)_{ij}$ from (18) and (20) we perform the time extrapolation by means of the formulas

$$\xi_{ij}(t + \Delta t) = \xi_{ij}(t - \Delta t) + 2\,\Delta t \left(\frac{\partial \xi}{\partial t}\right)_{ij}(t)$$

$$z_{ij}(t + \Delta t) = z_{ij}(t - \Delta t) + 2\,\Delta t \left(\frac{\partial z}{\partial t}\right)_{ij}(t)$$

except at the first step where uncentered time differences must be used. The entire process is repeated n times if a forecast is desired for the time $n\,\Delta t$.

V. The Computational Stability of the Finite Difference Equations

If the finite difference solution is to approximate closely the continuous solution, Δs and Δt must be small in comparison to the space and time scales of the physically relevant motions. But this does not alone insure accuracy; the small-scale motions for which there is inevitably a large distortion may possibly be amplified in the course of computation to such an extent that they will totally obscure the significant large-scale motions. In the following we shall derive the criteria which insure that no such amplification will take place. We shall employ a heuristic procedure which is, however, patterned after the rigorous method of COURANT, FRIEDRICHS, and LEWY (1928).

Since we are concerned with the behavior of small-scale, high-frequency perturbations, we may linearize the vorticity equation and assume the coefficients to be constant in a region which, though small, is yet sufficiently large to contain several of the small perturbations. If z' denotes a small perturbation superimposed on a smooth large-scale motion, the vorticity equation may be written

$$\frac{\partial}{\partial t}(\Delta z') = J(\eta, z') + hJ(\Delta z', z) + J(h, z)\,\Delta z' \qquad (22)$$

and we have to consider the computational stability of its finite difference analogue:

$$\Delta_{ij}\left[\frac{z'_{ij}(t + \Delta t) - z'_{ij}(t - \Delta t)}{2\,\Delta t}\right] = \frac{\partial \eta}{\partial x}\left(\frac{z'_{ij+1} - z'_{ij-1}}{2\,\Delta s}\right)\frac{\partial \eta}{\partial y}\left(\frac{z'_{i+1j} - z'_{i-1j}}{2\,\Delta s}\right) + h\,\frac{\partial z}{\partial y}\left(\frac{\Delta_{i+1j} z' - \Delta_{i-1j} z'}{2\,\Delta s}\right) - h\,\frac{\partial z}{\partial x}\left(\frac{\Delta_{ij+1} z' - \Delta_{ij-1} z'}{2\,\Delta s}\right) + J(h, z)\,\Delta_{ij} z', \qquad (23)$$

in which the coefficients of the terms in z' may be considered constant. If, as before, the boundary is rectangular, the perturbation may be expanded into a finite Fourier series and it is enough to take an individual harmonic of the form

$$z' = e^{i(kx + \mu y + \nu t)},$$

where

$$k = \frac{\pi l}{p\,\Delta s} = \frac{\pi l}{L_x}\ (l = 1, 2, \ldots, p - 1),$$

$$\mu = \frac{\pi m}{q\,\Delta s} = \frac{\pi m}{L_y}\ (m = 1, 2, \ldots, q - 1), \qquad (24)$$

ν is the frequency, which may be complex, and L_x and L_y are the x and y dimensions of the grid rectangle. Substitution into (23) then gives, after some manipulation of terms,

$$\frac{\omega - \omega^{-1}}{2} = ai + J(h, z)\,\Delta t, \qquad (25)$$

where

$$\omega = e^{i\nu \Delta t}, \qquad (26)$$

and

$$a = h\,\frac{\Delta t}{\Delta s}\left(\frac{\partial z}{\partial y}\sin k\,\Delta s - \frac{\partial z}{\partial x}\sin \mu\,\Delta s\right) - \frac{\Delta s\,\Delta t}{4}\cdot\frac{\frac{\partial \eta}{\partial x}\sin k\,\Delta s - \frac{\partial \eta}{\partial y}\sin \mu\,\Delta s}{\sin^2\frac{k\,\Delta s}{2} + \sin^2\frac{\mu\,\Delta s}{2}}. \qquad (27)$$

Clearly the disturbance will not amplify if $|\omega| \leq 1$. To investigate the conditions under which this is so, let us first consider (25)

without the term $J(h, z)\,\Delta t$. Put ω_0, a root of this equation, equal to $\varrho e^{i\Theta}$, where ϱ is positive and Θ real. $|\omega_0| = \varrho \leq 1$ is required for stability. Since $-\omega_0^{-1} = -\varrho^{-1} e^{-i\Theta}$ is a root along with ω_0, $\varrho \geq 1$ is also required. Hence $\varrho = 1$, $\omega_0 = e^{i\Theta}$, and

$$\omega_0 - \omega_0^{-1} = e^{i\Theta} - e^{-i\Theta} = 2i \sin \Theta,$$

and the stability condition becomes

$$|a| = |\sin \Theta| \leq 1. \tag{28}$$

To find an upper bound for $|a|$ we consider separately the two terms in (27). The absolute value of the first is bounded by

$$\sqrt{2}\,\frac{\Delta t}{\Delta s} \max |h \nabla z| = \sqrt{2}\,\frac{\Delta t}{\Delta s} \max |m \mathbf{v}|.$$

The second increases indefinitely in numerical value with diminishing k and μ, but it must be recalled that

$$k = \frac{\pi l}{L_x} \geq \frac{\pi}{L_x}$$

$$\mu = \frac{\pi m}{L_y} \geq \frac{\pi}{L_y}.$$

Since $k \Delta s$ is small, we may approximate the sine terms in the numerator and denominator by their arguments to obtain the upper bound

$$\Delta t \cdot \frac{L}{\sqrt{2}\,\pi} \max |\nabla \eta|,$$

where

$$L = \left[\frac{1}{2}\left(L_x^{-2} + L_y^{-2}\right)\right]^{-\frac{1}{2}}.$$

Hence the condition $|a| \leq 1$ leads to the stability criterion

$$\frac{\Delta s}{\Delta t} \geq \sqrt{2}\left(\max |m \mathbf{v}| + \frac{L \Delta s}{2\pi} \max |\nabla \eta|\right). \tag{29}$$

Consider now the effect of the term $J(h, z)\,\Delta t$ in equation (25). This equation (in ω) has no multiple roots except at $a = \pm 1$. If this is excluded, that is, if the stability condition is strengthened to $|a| < 1$, then the extra term in question will merely cause a change in ω of the order Δt. Over a time t, that is, over $t/\Delta t$ steps, this will lead to an accumulation of errors which does not increase indefinitely for Δt approaching zero. That is, this does not cause an amplification of error that can vitiate the convergence of an approximate solution to the true solution for Δt approaching zero. Thus, at most an irrelevant modification of the stability criterion may be called for; the exclusion of the equality sign in the inequality that defines a lower bound for $\Delta s/\Delta t$.

Because of the extreme approximative character of the derivation of (29) this stability criterion can be regarded only as a rough directive in the selection of Δs and Δt. In addition, the second parenthetical term on the right hand side of (29) originates from a term in a that is proportional to Δt and hence is comparable to the term $J(h, z)\,\Delta t$ whose neglect was advocated above. Finally the size of the L which enters here is debatable: To use the full L (i.e., L_x, L_y) seems uncalled for, since phenomena on the largest possible scale are not aimed at by these considerations. A detailed discussion of these factors would take us too far from principal subject. The actual values used for Δx and Δt were chosen on the basis of a combination of the above principles and general physical considerations and were ultimately justified when the computation was found to be stable.

VI. Presentation and Analysis of Results

The forecasts were computed for a period of 24 hours. The time interval used was at first one hour but was increased to two and then three hours when it was found that the larger intervals gave practically identical forecasts and did not lead to computational instability. The space interval Δs was taken to be 736 km, or 8 degrees of longitude at 45 degrees latitude on the map, and the grid rectangle consisted of 15×18 space intervals. An actual grid is shown in figure 1.

It will be seen that the distances are so great that good resolution cannot be expected for any but the largest scale motions. Unfortunately a smaller interval would too greatly have reduced the size of the forecast area, for the total number of grid points was restricted

by the limited internal memory capacity of the Eniac. It may be of interest to remark that the computation time for a 24-hour forecast was about 24 hours, that is, we were just able to keep pace with the weather. However, much of this time was consumed by manual and I.B.M. operations, namely by the reading, printing, reproducing, sorting, and interfiling of punch cards. In the course of the four 24 hour forecasts about 100,000 standard I.B.M. punch cards were produced and 1,000,000 multiplications and divisions were performed. (These figures double if one takes account of the preliminary experimentation that was carried out.) With a larger capacity and higher speed machine, such as is now being built at the Institute for Advanced Study, the non-arithmetical operations will be eliminated and the arithmetical operations performed more quickly. It is estimated that the total computation time with a grid of twice the Eniac-grids density, will be about $^1/_2$ hour, so that one has reason to hope that RICHARDSON'S dream (1922) of advancing the computation faster than the weather may soon be realized, at least for a two-dimensional model. Actually we estimate on the basis of the experiences acquired in the course of the Eniac calculatons, that if a renewed systematic effort with the Eniac were to be made, and with a thorough routinization of the operations, a 24-hour prediction could be made on the Eniac in as little as 12 hours.

Insofar as possible, weather situations were chosen in which the changes of interest occurred over North America or Europe, the areas with the best data coverage. It must be borne in mind, however, that forecasts for the western coasts are reduced somewhat in accuracy by lack of data in the Pacific and Atlantic oceans.

The data were taken from the conventional 500 mb analyses of the U. S. Weather Bureau and were accepted without modification in interpolating for the initial values of z at the grid points. It was realized that the conventional analyst pays more attention to wind direction than to wind speed and more attention to directional smoothness of the height contours than to their spacing, but it was thought that the more or less random errors introduced in this way would be smoothed out in the integration. Unhappily this was not always so, and it now appears that an objective analysis would have been preferable.

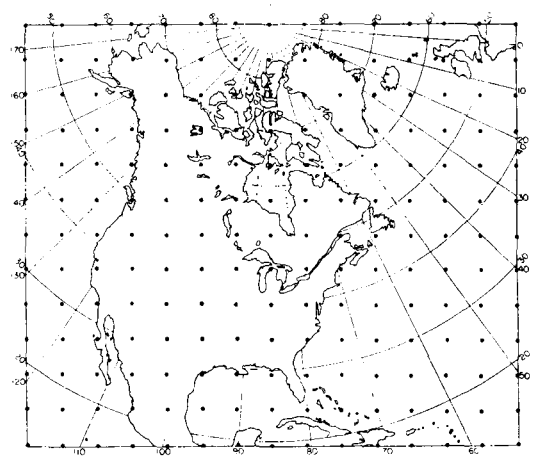

Fig. 1. A typical finite-difference grid used in the computations. A strip two grid intervals in width at the top and side borders and one grid interval in width at the lower border is not shown.

The forecasts were made from the 0300 GMT 500 mb charts for January 5, 30, and 31, and February 13, 1949. On these dates the weather systems were of so large an amplitude that their development could not have been explained by small perturbation theory or by simple translation. Each forecast is illustrated by four diagrams (fig. 2—5): (a) contains the initial height contours in units of 100 ft and the initial isolines of absolute vorticity in units of $1/3 \times 10^{-4}$ sec^{-1}; (b) contains the observed height contours and constant absolute vorticity lines 24 hours later; in (c) the contours of observed height change in hundreds of feet are shown as continuous lines and the contours of predicted height change as broken lines; (d) shows the predicted height contours and constant absolute vorticity lines.

The spurious boundary influences were removed, by excluding from the drawings a strip adjacent to the boundaries which was two grid intervals in width at the west, east, and north boundaries, and one grid interval in width at the south boundary where the influence velocities were smaller.

The forecast of January 5, in which the principal system was an intense cyclone over the United States, was uniformly poor. The forecast gave much too small a displacement

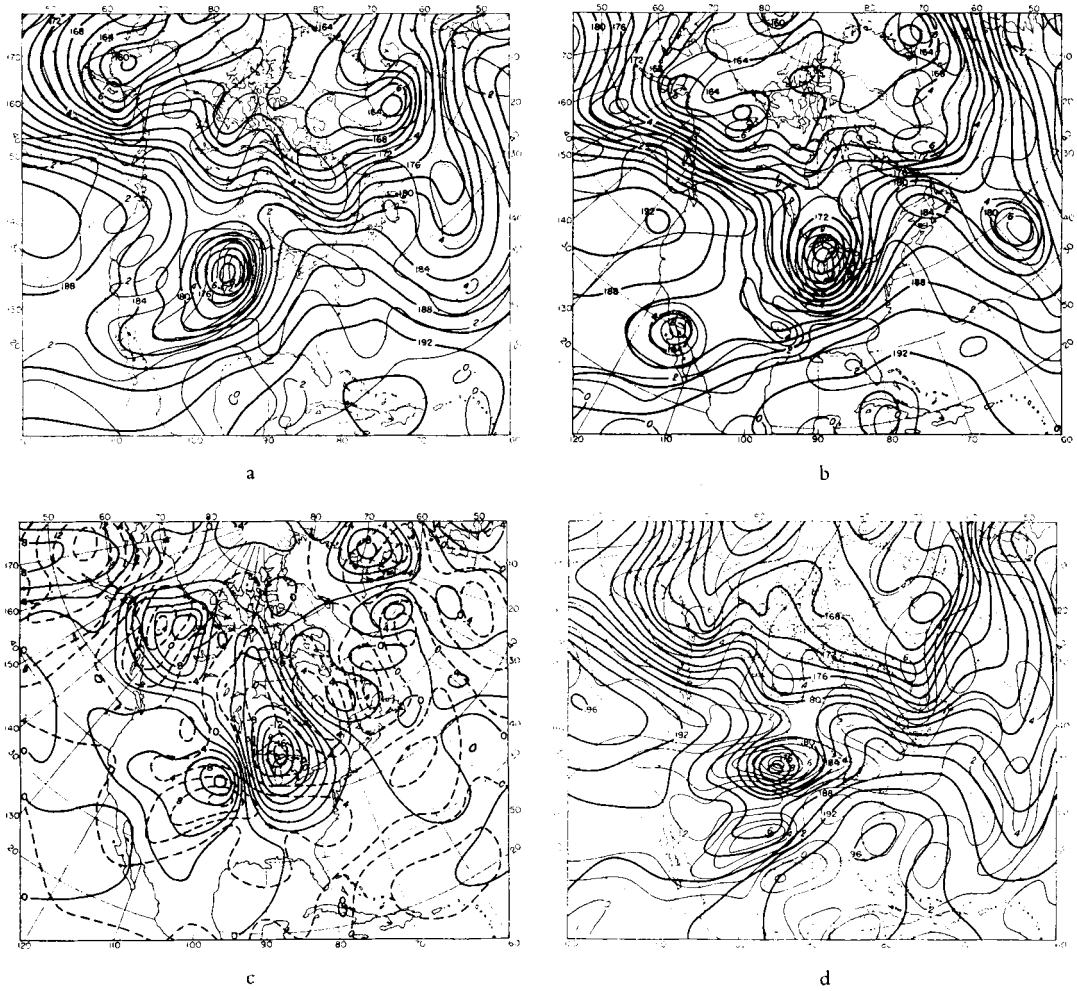

Fig. 2. Forecast of January 5, 1949, 0300 GMT: (a) observed z and η at $t = 0$; (b) observed z and η at $t = 24$ hours; (c) observed (continuous lines) and computed (broken lines) 24-hour height change; (d) computed z and η at $t = 24$ hours. The height unit is 100 ft and the unit of vorticity is $1/3 \times 10^{-4}$ sec^{-1}.

of the cyclone and also distorted its shape, and the predictions of the other motions were equally inaccurate. On the other hand, the January 30 forecast contained a number of good features. The displacement and amplification of the trough over the United States at about 110° W was well predicted, as was the large scale shifting of the wind from NW to WSW and the increase in pressure over eastern Canada. The displacement of the axis of the major trough over the eastern United States and Canada was correctly predicted, but the strong circulation that developed at its southern extremity was not. Proceeding eastwards we find that the amplification of the trough over the North Sea together with the characteristic breakthrough of the northwesterly winds and the corresponding destruction over France of the eastern nose of the anticyclone was predicted approximately. This is shown by the agreement of the predicted with the observed height changes over western Europe. On the next day the forecast was even better; the continued turning of the northwesterly winds over the North Sea and their extension into southwestern Europe was correctly predicted. The major discrepancy was the appearance of a sharp anticyclonic ridge south of Newfound-

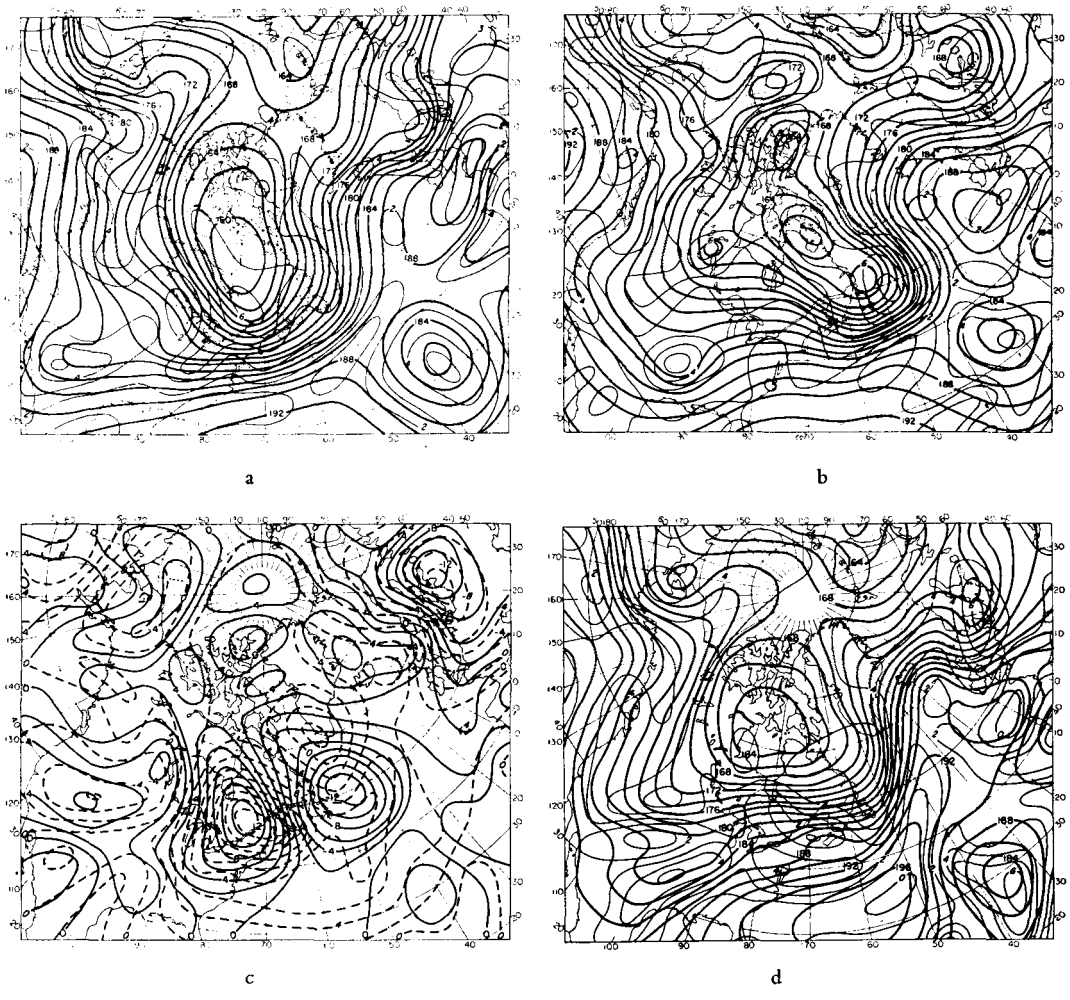

Fig. 3. Forecast of January 30, 1949, 0300 GMT. (See Fig. 2 for explanation of diagrams.)

land, which is also indicated by the excessive observed pressure rises over Newfoundland. We note, however, that the position of the center of these rises was correctly predicted. On February 13 the major changes occurred at the west coast of North America and in the Atlantic Ocean and were consequently difficult to forecast and to verify. Too great consideration should not be given to the Atlantic forecast, since data for this area were virtually non-existent.

An attempt will now be made to account for the errors in the forecasts. The success of such an attempt will, of course, depend upon one's ability to separate the computational and analysis errors from those which were due to defects in the model. This unfortunately will not always be possible. Because of the excessive size of the space increments, the computational errors were in some instances obviously so great that nothing definite could be said about the residual errors due to the shortcomings of the model. The January 5 forecast was a case in point. Here the grid interval was not at all small in comparison with the scale of the systems, and one had to expect a large computational error. This was not equally true of the remaining forecasts where the scale

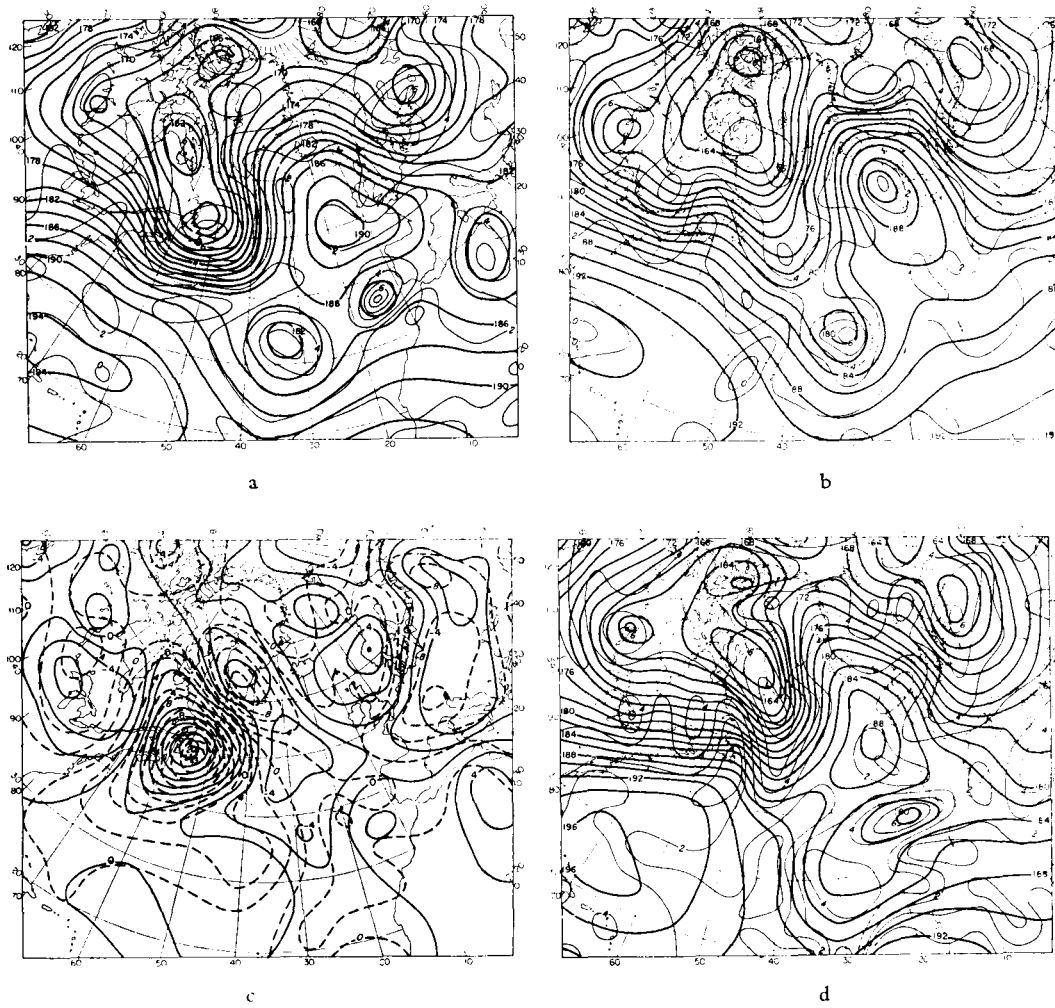

Fig. 4. Forecast of January 31, 1949, 0300 GMT. (See Fig. 2 for explanation of diagrams.)

was in general considerably greater. Errors in analysis also contributed to the difficulty in interpreting the results of the forecasts. These will be minimized as far as possible by confining the discussion to areas in which the analysis was fairly reliable. Ultimately, however, the importance of the analysis errors can be accurately judged only by making a series of forecasts with the same data but with varying independent analyses, both subjective and objective. In view of the above mentioned difficulties the following discussion must be regarded as highly tentative.

1. *Truncation errors. (Errors due to the replacement of the [strict] differential equation by an [approximant] difference equation.)* — Examples of unsystematic errors due to truncation are found by comparing the verification map for January 30 (fig. 3 b) with the synoptically identical initial map for January 31 (fig. 4 a). The difference in position of the grids is reflected in differing absolute vorticity patterns. Because of the large scale character of the systems the discrepancies are on the whole not great. Some are connected with the slight uncertainty in the actual drawing of the absolute vorticity lines. However, it is seen that there is a large discrepancy in the two patterns around the low off the west coast of Portugal: on the one map absolute vorticities of greater than

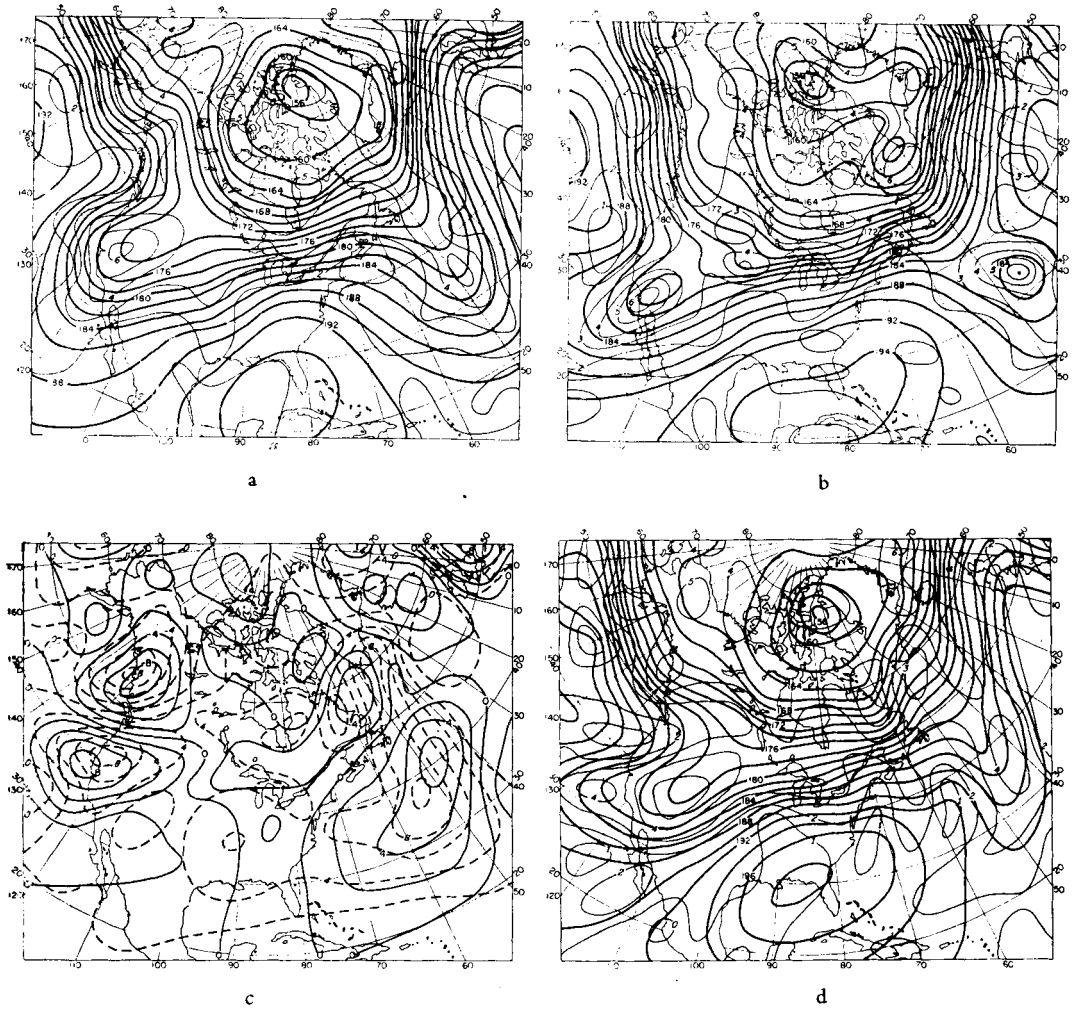

Fig. 5. Forecast of February 13, 1949, 0300 GMT. (See Fig. 2 for explanation of diagrams.)

7 units were measured, whereas on the other the greatest measured absolute vorticity was but 4 units.

According to the basic assumption underlying the computations one should expect to find that the absolute vorticities "move with the fluid". Merely by inspecting the map for January 5 it becomes clear that it is impossible to account for some of the major changes in the pattern of absolute vorticity around the low over the United States from the advection of absolute vorticity. Truncation errors have here to a large extent influenced the results and are probably the main reason for the strange computed deformation of this low.

The assumption of the conservation of absolute vorticity requires in particular that the extreme values of the absolute vorticity remain unchanged. An inspection of the individual minima brings out the fact that nearly all of them intensified during the computation (a similar computational error did not occur for the maxima). These discrepancies account for some of the main errors in the forecast. Thus on January 31 the maximum height increase, which is found over Newfoundland, was about 600 ft. too great but corresponding to this there was a rather large decrease in absolute vorticity that cannot possibly be accounted for by advection. A

similar fictitious decrease of vorticity on February 13 off the east coast of the United States may very likely have been responsible for the exaggerated height increase in the Atlantic.

A comparison between computed and observed displacements of well-defined troughs and ridges gave the result that out of 20 troughs 16 moved too slowly and the rest with about the right speed, and of 10 ridges 5 moved too slowly, 3 too fast, and 2 about right. Thus on the whole the disturbances were computed to move too slowly. The discrepancy is apparently not due to truncation error since the finite difference approximation does not systematically underestimate the wind speed. Nor is the explanation to be found in the geostrophic assumption. The geostrophic wind is a poor approximation to the actual wind in regions where the height contours are strongly curved; but the winds are overestimated in cyclones and underestimated in anticyclones, and this is just the contrary of what must be true if the computed motions are to be explained. A possible explanation is given by the fact already mentioned in Section II that the level of nondivergence is probably higher than 500 mb. If this level were appreciably higher, the speed of propagation would increase significantly because of the greater speed of the wind.

2. *Errors due to non-fulfillment of the vertical wind variation assumption.* — The approximation (1) that the winds are parallel at all heights is admittedly a crude one. An indication of how the motion is modified when this assumption is dropped is given by the following consideration.

We replace (1) by the synoptically more tenable assumption that the isotherms are parallel at all heights. In particular, we assume that $\mathbf{v}$ may be written

$$\mathbf{v} = \overline{\mathbf{v}} + \mathbf{v}_T, \tag{30}$$

where $\overline{\mathbf{v}}$ is the mean wind, supposed equal to the actual wind at $p = \bar{p}$, and $\mathbf{v}_T$ is the thermal wind referred to this level.

With slight approximation the vertically averaged vorticity equation may be written[6]

$$\overline{\frac{d}{dt} \ln (\zeta + f)} \approx 0,$$

or, since $f \gg \zeta$, except near the center of an intense cyclone,

$$\frac{\partial \overline{\zeta}}{\partial t} = -\overline{\mathbf{v} \cdot \nabla \eta}. \tag{31}$$

Inserting the expression (30) and noting that by definition $\overline{\mathbf{v}}_T = 0$, we obtain

$$\frac{\partial \overline{\zeta}}{\partial t} = -\overline{\mathbf{v}} \cdot \nabla (\overline{\zeta} + f) - \overline{\mathbf{v}_T \cdot \nabla \zeta_T} \tag{32}$$

where ζ_T is the vorticity of the thermal wind.

If $\mathbf{v}_T$ were parallel to $\overline{\mathbf{v}}$ we should again obtain equation (3), but the interesting case is where the isothermal pattern is out of phase with respect to the streamline pattern. In this case the last term in (32) produces vorticity changes which lead to an increase or decrease in the total kinetic energy. In the special case of a symmetric trough with a north-south axis, this term gives an increase of cyclonic vorticity along the axis when the isotherm trough is displaced towards the west. The increase of absolute vorticity in the major trough near the east coast of Canada on January 30 may thus be attributed to a phase lag of the isotherm pattern which was observed at 0300 GMT. As this development was the principal discrepancy in what was otherwise a good forecast, an attempt is made at the close of this article to give a quantitative explanation in terms of a simplified baroclinic model.

3. *The effects of baroclinicity.* — The most typical conditions for the breakdown of the barotropic model will probably occur when potential energy is converted into kinetic energy. This usually is reflected in the intensification of the extrema of absolute vorticity which, as remarked earlier, is inconsistent with the assumption of conservation of absolute vorticity in a horizontal non-divergent flow. Therefore, an inspection of the observed changes at the extreme points in the field of η can be expected to give some information as to what extent the model has applied in the present situations. As a further test the initial and verification maps may be consulted to ascertain whether areas enclosed within isolines of absolute vorticity were actually conserved, and whether such regions if initially simply connected remained so in the observed developments. The February 13 forecast offers

[6] CHARNEY (1948).

two typical examples of the failure of the model in this sense. In the trough over the east coast of the Hudson Bay the maximum absolute vorticity was initially between 5 and 6 units but became, after 24 hours, closer to 7 units, corresponding to the observed, but not predicted, intensification of the trough. The other example is the trough over the west coast of the United States. Here the region with the isolines of absolute vorticity labeled by 4 was split into two separate regions in the observed development, and this splitting was confirmed even more markedly when the absolute vorticities were recomputed for a finer grid. The corresponding destruction of vorticity was responsible for the cutting off of a closed low which the computations failed to give.

4. *Barotropy versus baroclinicity.* — It should be clear that the fact that vorticity may be created or destroyed cannot annihilate the physical effects from the horizontal transport of vorticity. The problem is to determine the relative importance of these effects in comparison with those resulting from the action of forces creating or destroying circulation. The following points of view may be put forth in the light of the results of the present forecasts. Considering first the barotropic effects, it may be said that these were seldom if ever negligible in magnitude compared with the observed changes and were often the predominating ones. Moreover the transport of vorticity did not contribute merely to the translational propagation of systems but also to their development by the dispersion of kinetic energy. The forecasts for January 30 and January 31 are illustrations of this point.

As to the effect of the non-conservation of absolute vorticity, the evidence, both from the observed developments and from the failure of the forecasts in a number of instances where the error could not be attributed to the use of finite differences, supports the commonly accepted view that baroclinicity cannot be ignored even in day to day changes in the upper flow patterns. Even when small, the non-barotropic effects may be responsible for important structural changes in the velocity field, as for example, in the cutoff low on January 13. However, this importance is not everywhere and at all times the same. Baroclinic effects were apparently decisive in determining the development of the major trough over eastern Canada and the United States on January 30 as the trough moved into the Atlantic, but on the following day the greatest part of the change was accounted for by the transport of the absolute vorticity.

In addition to the independent effects of barotropy and baroclinicity there is also the problem of their mutual interaction. An intrusion of vorticity in one locality, by changing the velocity field, automatically changes the conditions for the advection of vorticity in the surroundings. In this sense the addition of even small vorticities may be important, especially in regions of intense extrema of absolute vorticity. These regions generally possess large amounts of kinetic energy, and small changes in the vorticity field may produce large changes in the vorticity advection. The motion of the intense low over the United States on January 5 was possibly an example of this effect. From an inspection of the initial map it is seen that the height contours and isolines of absolute vorticity coincided to a high degree, whereas on the observed map 24 hours later the center of absolute vorticity was displaced slightly to the south of the center of the low pressure, thus giving more favorable conditions for the displacement of the whole system. Actually it was found from the observed map for 1500 GMT that the center speeded up in the second half of the 24-hour period.

We may add that while baroclinic effects may be important in changing the conditions under which advection of absolute vorticity takes place, barotropic effects may distort the mass field and thereby influence the conditions under which potential energy is converted into kinetic energy. It is not, however, within the scope of this paper to discuss such effects, as little light can be thrown upon them by a study of purely barotropic processes.

5. *Suggestions for the improvement of the barotropic forecasts.* — Strictly speaking the quasi-barotropic equation that has been used applies to the vertically averaged motion of the atmosphere. If, therefore, the actual motion at the level whose motion most closely approximates the mean has superimposed upon it other motions that do not appear in the vertical average, these motions will not be

governed by the equation of mean motion and will consequently exert a distorting effect on the forecasts. Hence, if it is possible in some approximate sense to ascribe to these motions a quasi-independent behavior, it would seem preferable to forecast the mean motions themselves and then to identify the mean motions with those at a particular level, rather than to operate with the motions for this level from the beginning. Thus it is suggested that errors due to motions that do not satisfy (1), as well as analysis errors, may be reduced by defining the $z^\star$ in

$$\Delta_s \frac{\partial z^\star}{\partial t} = J_s\left(\frac{g}{f}\Delta_s z^\star + f, z^\star\right) \quad (33)$$

by

$$z^\star = \frac{A^\star}{\bar{A}} z = \frac{A^\star}{\bar{A}} \cdot \frac{1}{p_o}\int_0^{p_o} z\, dp \quad (34)$$

instead of by z at the level $p^\star$.

It is, of course, obvious that the length of the space interval should be reduced in future forecasts, but care must then be exercised in selecting the method of interpolation of the grid values. If the interpolation were performed subjectively, decreasing the size of the grid interval would lead to increasingly large errors in the difference quotients because of the increasing difficulty in determining small differences by subjective estimation. One might argue that a very small interval should not in any case be used because it would exaggerate the noise motions. But the way to smooth these motions is not to use a grid interval that distorts the large-scale motions; the smoothing is much more efficiently and exactly accomplished by fitting the data by polynomials or other mathematical functions which can be chosen in advance to give any desired degree of smoothing. A reduction in the size of the grid interval would then give more rather than less accuracy in approximating a derivative by a finite difference quotient.

6. *A simplified baroclinic model.* — In an effort to assess the relative importance of pure advection of absolute vorticity as against the circulation producing forces of the atmosphere, the following baroclinic model has been adopted because of its simplicity and adaptability to numerical analysis. It is also put forward as the next in a hierarchy of models whose study is expected to lead to a better understanding of the atmospheric motions. The essential simplification has been brought about by the geostrophic assumption and the assumption of horizontal advection of potential temperature. As it turns out, the reasoning is much in accord with that of SUTCLIFFE (1947, 1950).

If pressure is adopted as a vertical coordinate, the hydrostatic equation may be written

$$\frac{\partial z}{\partial p} = -\frac{1}{g\varrho} \quad (35)$$

from which one derives

$$\frac{\partial}{\partial p}\left(\frac{\partial z}{\partial t}\right) = -\frac{1}{g\varrho}\frac{\partial \ln \vartheta}{\partial t}, \quad (36)$$

where ϑ is the potential temperature. Integration from p_o, the pressure at the ground, to an arbitrary level p and application of the surface spherical Laplacian operator to both sides of the resulting equation then gives

$$\Delta_s\left(\frac{\partial z}{\partial t}\right) = \Delta_s\left(\frac{\partial z}{\partial t}\right)_o + \Delta_s A \quad (37)$$

where the subscript o denotes a surface value, and

$$A = -\int_{p_o}^{p} \frac{1}{g\varrho}\frac{\partial \ln \vartheta}{\partial t}\, dp.$$

Taking the vertical pressure average we get

$$\Delta_s\left(\frac{\partial \bar{z}}{\partial t}\right) = \Delta_s\left(\frac{\partial z}{\partial t}\right)_o + \Delta_s \bar{A} \quad (38)$$

The terms $\Delta_s\left(\frac{\partial z}{\partial t}\right)_o$ and $\Delta_s\left(\frac{\partial \bar{z}}{\partial t}\right)$ may now be eliminated between (37), (38), and (31) in the form

$$\Delta_s\left(\frac{\partial \bar{z}}{\partial t}\right) = \bar{J}_s(\eta, z), \quad (39)$$

to give

$$\Delta_s\left(\frac{\partial z}{\partial t} + A - \bar{A}\right) = \bar{J}_s(\eta, z) \quad (40)$$

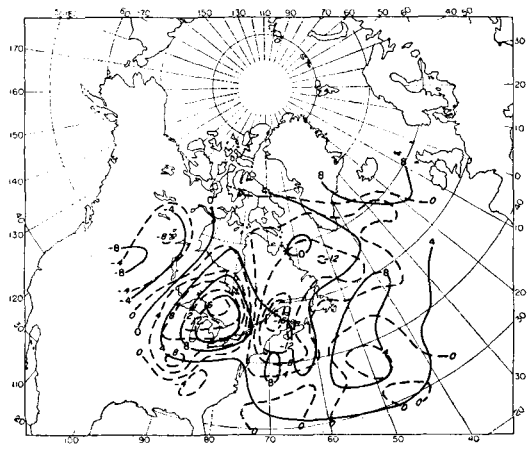

Fig. 6. Barotropically and baroclinically computed 500 mb height tendencies at 0300 GMT, January 30, 1949. The barotropic tendencies are represented by continuous lines and the baroclinic tendencies by broken lines. The unit is 100 ft/24 hours.

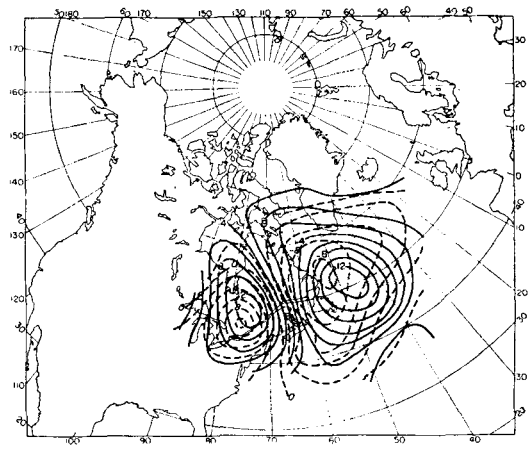

Fig. 7. The broken lines represent the 24-hour height change computed by translating the baroclinically computed tendency field shown in Figure 6 in the direction of the mean current and with the speed of the trough. The solid lines represent the observed 24-hour height change.

The advective hypothesis is finally introduced by ignoring w in the approximate adiabatic equation

$$\frac{\partial \ln \vartheta}{\partial t} = -\mathbf{v} \cdot \nabla \ln \vartheta - \frac{w}{g\varrho} \frac{\partial \ln \vartheta}{\partial p}, \quad (41)$$

and substituting the resultant expression for $\partial \ln \vartheta / \partial t$ in A.

Equation (40) is then seen to be a generalization of the quasi-barotropic equation (3), for if the assumption (1) is made, streamlines and isolines are everywhere parallel, and $A = \bar{A}$ at the level $\bar{p}$. It also can be shown to reduce to (32) under the assumption (30). Its solution is obtained as before by solving a Poisson's equation in two dimensions.

Equation (40) has been applied to the computation of the initial height tendency for the January 30 situation as a means of explaining the major discrepancy in the barotropic forecast for that date. The vertical integrations needed for evaluating $\bar{J}(\eta, z)$, and $\bar{A}$ were based on data obtained from the 1000, 850, 700, 500, 300, 200, and 100 mb charts.

It was to be expected that the advective hypothesis would be found untenable in the stratosphere because of the great statical stability there. Indeed, it turned out that the tendencies were greatly improved by ignoring entirely the local potential temperature changes in the stratosphere, i.e., by assuming that the change in potential temperature due to horizontal advection is exactly compensated by its vertical transport. On this basis the initial height tendencies were calculated for all levels up to 300 mb for a region containing the trough at the east coast of Canada and United States. The 500 mb tendencies are shown in fig. 6 together with the computed initial tendencies obtained from the barotropic model. The units are in hundreds of feet per 24 hours. It is immediately apparent that the baroclinically calculated height falls on the east side of the trough are more favorable, both with respect to intensity and position, for the observed development. In order to obtain a more direct comparison with observation, the computed baroclinic tendency field was translated for 24 hours with the past speed of the trough in the direction of the mean current. The resulting 24-hour height change, together with the observed height change, is shown in fig. 7. It is seen from the diagram that the correspondence is close and by comparison with fig. 3 is much better than the barotropically computed change.

It may also be mentioned that the computed baroclinic tendencies for the 1000 mb level

corresponded reasonably well with the observed tendencies on the sea-level map. The pressure falls to the northeast of a well developed surface cyclone were, if anything, somewhat too great. An effort is now being made to see whether the effect of vertical motions is to reduce the falls. Some preliminary calculations indicate that this is the case.

Acknowledgments

The writers wish to thank Mrs K. VON NEUMANN for instruction in the technique of coding for the Eniac and for checking the final code, Professor G. PLATZMAN of the University of Chicago for his considerable help and advice in coding the computations for the Eniac, Mr J. FREEMAN of the Meteorological Research Group at the Institute for Advanced Study and Mr J. SMAGORINSKY of the U. S. Weather Bureau for their assistance in the preliminary work of data preparation and in the actual running of the computations on the Eniac at Aberdeen. Professor PLATZMAN also participated in the work at Aberdeen, where again his advice proved most valuable. We are also greatly obliged to the staff of the Computing Laboratory of the Ballistic Research Laboratories for help in coding the problem for the Eniac and for running the computations.

REFERENCES

CHARNEY, J. G., 1948: On the scale of atmospheric motions. *Geofys. Publ.*, **17**, 2, 17 pp.

CHARNEY, J. G., 1949: On a physical basis for numerical prediction of large-scale motions in the atmosphere. *J. Meteor.*, **6**, 6, 371—385.

CHARNEY, J. G. and A. ELIASSEN, 1949: A numerical method for predicting the perturbations of the middle latitude westerlies. *Tellus*, **1**, 2, 38—54.

COURANT, R., K. FRIEDRICHS, and H. LEWY, 1928: Über die partiellen Differentialgleichungen der mathematischen Physik. *Math. Ann.*, **100**, 32—74.

RICHARDSON, LEWIS F., 1922: *Weather prediction by numerical process.* Cambridge University Press. 236 pp.

SUTCLIFFE, R. C., 1947: A contribution to the problem of development. *Quart. J. R. Meteor. Soc.*, **73**, 317—318, 370—383.

SUTCLIFFE, R. C. and A. G. FORSDYKE, 1950: The theory and use of upper air thickness patterns in forecasting. *Quart. J. R. Meteor. Soc.*, **76**, 328, 189—217.